

Temporal Evolution of Impurity Profile Measured by a Soft X-ray Detector Array on LHD

OHDACHI Satoshi*, YAMAMOTO Satoshi¹, TAKECHI Manabu¹, TOI Kazuo, GOTO Motoshi, KAWAHATA Kazuo, KOBUCHI Takashi, MORITA Shigeru, MUTO Sadatsugu, NARIHARA Kazumichi, PETERSON Byron J., SATO Kuninori, TANAKA Kenji, TOKUZAWA Tokihiko, YAMADA Ichihiko and LHD Experimental Group 1 and Group 2

National Institute for Fusion Science, Toki 509-5292, Japan

¹*Dep. of Eng. Science, Nagoya Univ., Nagoya 464-01, Japan*

(Received: 18 January 2000 / Accepted: 20 July 2000)

Abstract

A stable method to reconstruct the soft X-ray (SX) emissivity profile is described in detail from the measurements of the SX detector array system on the Large Helical System (LHD). Sudden peaking of the SX emissivity profile after hydrogen ice-pellet injection is discussed, as an interesting application of this reconstruction method.

Keywords:

SX radiation, tomography, impurity accumulation

1. Introduction

Control of impurities is one of the important issues to realize a fusion reactor. On the Large Helical Device (LHD, $R/\bar{a} = 3.9$ m/0.6 m), discharges are often terminated by the radiation collapse when a discharge duration is fairly long (e.g. several tens of seconds). Degradation of plasma performance by contamination of impurities will be more serious issue in steady state plasmas. Measurements of detailed profiles of impurities are needed to clarify the impurity transport phenomena. We make use of SX radiation (SXR) profiles measured by an SX detector array system to obtain information of the impurity contents.

Experimental setup is described in Sec. 2 and a method to reconstruct the local emission is discussed in Sec. 3. The impurity radiation profile in a ice-pellet injected plasma is analyzed in Sec. 4 by the reconstruction method described in Sec. 3. Finally, the results are summarized.

2. Experimental Setup

A linear array of PIN photodiodes (developed by Kyoto Univ. [1] and Hamamatsu Photonics K.K.) is used as an SXR detector. The array contains 20 detectors. Each detector has a 12 mm × 1.5 mm active area and is separated with a center-to-center spacing of 2.25 mm. The upper limit of the frequency response is about 300 kHz. These signals are recorded by 14bit CAMAC ADCs with 10 kHz ~ 2 MHz sampling rates. Two sets of the arrays are installed on the top port of LHD (3.5U and 6.5U). The vertically elongated section of LHD plasma is covered by 40 sightlines with this system (Fig. 1). Typical space resolution Δr at the equatorial plane is 50 mm for the present aperture (2 mm × 6 mm). A Be foil with 15 μ m thickness is used to eliminate visible light (the cutoff energy of 15 μ m foil is about 1.3 keV).

*Corresponding author's e-mail: ohdachi@nifs.ac.jp

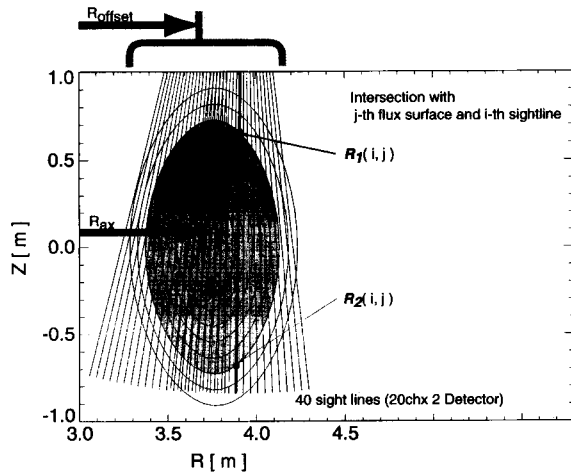


Fig. 1 Schematic view of the soft X-ray measurements in LHD.

3. Reconstruction of Emissivity Profile

Reconstruction of the SX emissivity P as a function of the normalized minor radius ρ is needed to study the impurities contents of a plasma. We propose a new method which determines the position of the magnetic surfaces and the SX emissivity P , simultaneously. We will explain the procedure by two steps.

3.1 Step1: Inversion of line integrated SX emissivity

If we assume that the SX emissivity is homogeneous on each flux surface, the measured signal of the i -th channel isx_i can be written by a linear combination of the emitted power p_j from the plasma inside the j -th flux surface:

$$\mathbf{I} = \mathbf{H} \mathbf{P} \quad (1)$$

where $\mathbf{I} = (isx_1, isx_2, \dots, isx_{N_{ch}})$ and $\mathbf{P} = (p_1, p_2, \dots, p_{N_{shell}})$. \mathbf{H} is an $N_{ch} \times N_{shell}$ matrix and is determined by the geometrical condition; $H(i, j) \propto \sqrt{(\mathbf{R}_1 - \mathbf{R}_2)^2}$, where, $\mathbf{R}_1(i, j)$ and $\mathbf{R}_2(i, j)$ are position vectors at the intersections of the i -th sightline with the j -th flux surface (see, Fig. 1).

Equation (1) can be solved by an iterative method. An initial emission profiles is assumed to be \mathbf{P}_0 . The emissivity vector \mathbf{P} is revised iteratively by $\Delta\mathbf{P}$, which is the solution of the following equation: $\mathbf{I} - \mathbf{H}'\mathbf{P} = \mathbf{H}'\Delta\mathbf{P}$. This iterative way is stabler than the simple way where Eq. (1) is directly solved.

We should determine the adequate number of the flux surface shells (N_{shell}) used in the calculation. The concept of AIC (Akaike's Information Criterion) may be

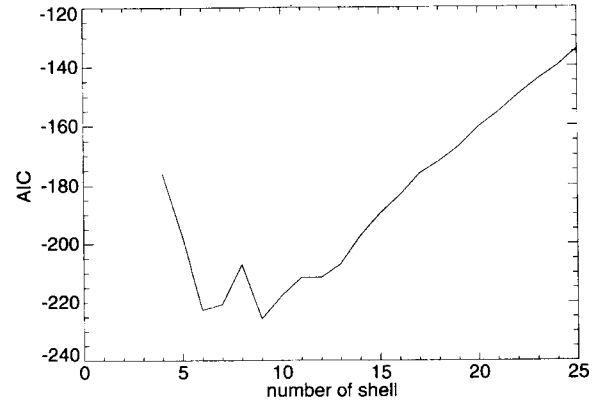


Fig. 2 AIC as a function of the number of the shells. It has a local minimum around $N_{shell} = 10$.

a guiding principle in this analysis. When the least square method is employed, the value of AIC is estimated as [2],

$$AIC \sim n \log S + 2r, \quad (2)$$

where n is the number of fitted data ($= N_{ch}$), S is the squared sum of residual error and r is the number of parameters ($= N_{shell}$). AIC as a function of N_{shell} is shown in Fig. 2. There is always a local minimum around $N_{shell} = 10$ experimentally suggesting that the best model is achieved with $N_{shell} = 10$. It is a reasonable result; considering the extent of the sightlines ($\Delta r = 50$ mm), the covering area of the adjacent sightlines are overlapped. The minor radius at a vertically elongated section a_{vert} is about 0.45 m and can be covered by 9 ($= a_{vert}/\Delta r$) sightlines. In other words, emission profiles at 10 (or 9) different positions give the maximum information we can extract from our profile data. We fixed that $N_{shell} = 10$ in analyses. The reconstructed image with $N_{shell} = 10$ is usually very smooth and do not contain negative values.

3.2 Step2: Determination of the shape of the flux surfaces

The second step is to determine the positions of flux surfaces. Flux surfaces with no plasma can be calculated exactly. However, after the plasma is produced, the flux surfaces are moved outward by the finite pressure of the plasma. The outermost surface is scraped off one after another at the ergodic magnetic layer which surrounds the closed flux surface region. The flux surfaces in a finite- β plasma is therefore smaller than those in vacuum field and the magnetic axis is shifted outward. We do not expect a good

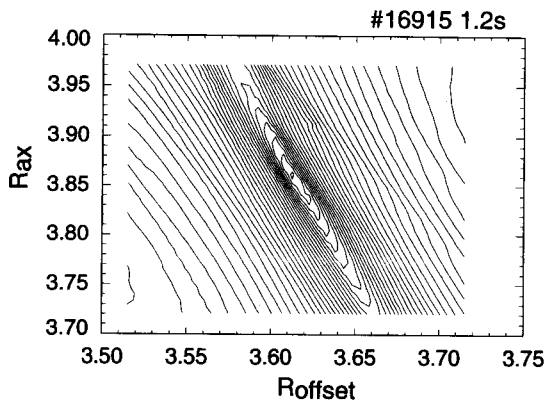


Fig. 3 Contour plot of the squared sum of the residual errors. The local minimum can be seen at $R_{\text{offset}} = 3.62$, $R_{\text{ax}} = 3.85$.

reconstruction using the flux surfaces of the vacuum magnetic field. More rigorous calculation using the equilibrium code (VMEC) with the measured pressure profile is, however, unrealistic since it takes so much CPU time.

We adopt a simple way to calculate the flux surfaces. On the assumption that the shape of the flux surface is not changed so much, we introduce two parameters to represent the shift of the magnetic surfaces of a plasma. One is the radial shift of the whole volume (R_{offset} , see Fig. 1) and the other is the shift of the magnetic axis (R_{ax}). With these two parameters, one can express most effect of the Shafranov shifts. Two parameters are determined where the residual errors are the minimum in the procedure described in Sec. 3.1. The squared sum of the residual errors are shown in Fig. 3 as a function of R_{offset} and R_{ax} . The local minimum can be seen in most cases. The structure of the local minimum is usually a simple one (Fig. 3). It is easy to determine the two parameters.

The magnetic axis and the outermost flux surface are also determined in this way independent of the equilibrium calculation; we can use the result for cross-checking of the equilibrium calculation. Calculated position of the magnetic axis and the boundary position agree well with the equilibrium calculation in low beta plasmas ($\beta_i < 1\%$).

4. Application of the Method

It is convenient to express the SX emissivity in term of the enhancement factor ζ . It is the ratio of the measured radiation to the bremsstrahlung emission for the pure hydrogen plasma. ζ is a good measure of the

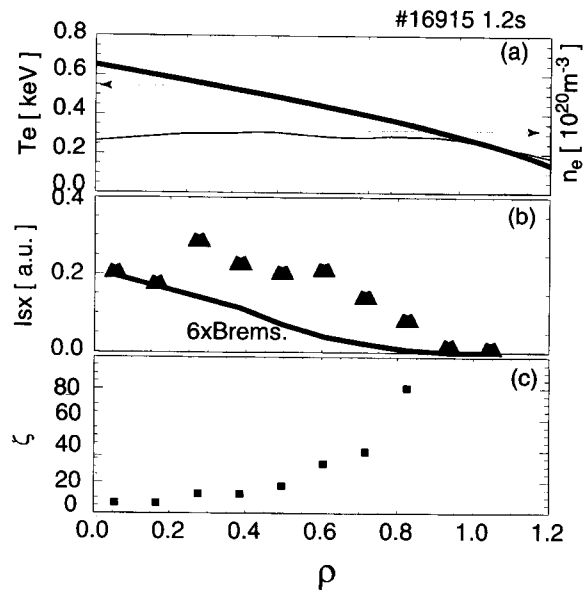


Fig. 4 Electron temperature and density profiles (a), reconstructed emissivity profile (triangles) and calculated bremsstrahlung profile (b) from $T_e(\rho)$, $n_e(\rho)$, enhancement factor ζ (c) are shown as a function of normalized minor radius ρ .

impurity contamination, since the SX emissivity will be increased by the recombination radiation and by the line radiation of the impurities. We calculate ζ using the electron temperature profile by a YAG thomson scattering system and the electron density by an FIR interferometer. An example of the ζ profile is shown in Fig. 4. The value of ζ is found to be 6 at the center. It varies (2 ~ 80) with plasma conditions. It has a strong dependence on the electron density. It is a decreasing function with the density [3].

Another example of the measurement in a pellet injected plasma (Fig. 5) is shown in Fig. 6. Measured profile becomes more peaked after 1 s. From 1.0 s to 1.5 s, the electron density and the electron temperature profiles are remain unchanged. Thus the change in SX emissivity profile would be caused by the change of the impurity content of the plasma. Since the total amount of impurities does not increase significantly (Change of the influx of metal impurities is very small, as is shown in Fig. 5), the transport of impurities may be changed. This type of sudden change of impurities transport occurs under various condition, e.g., pellet injection (this case), re-heat mode [4], and short interruption of NBI pulse. The physical mechanisms are not yet clarified.

Comparison between the results in this paper and

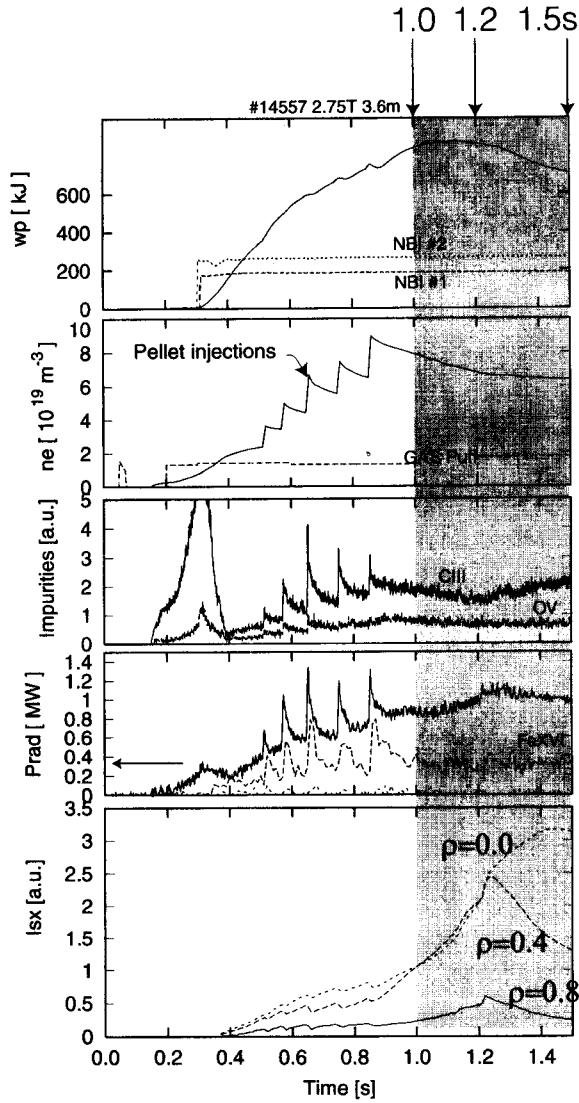


Fig. 5 Plasma parameters of # 14557. Impurity radiation profile is peaked in the hatched time window.

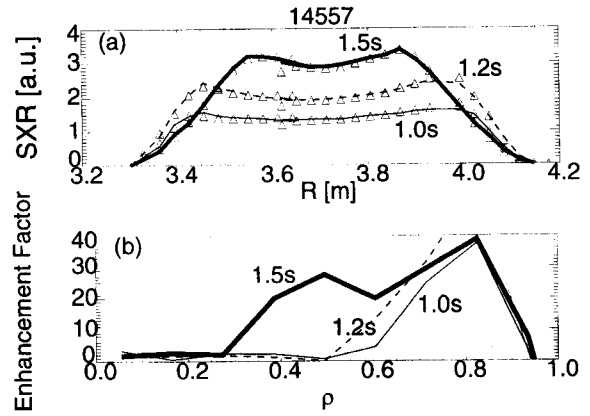


Fig. 6 SXR profile (a) and Enhancement factor profile (b) at 1.0 s, 1.2 s and 1.5 s in the plasma show in Fig. 5.

those from an impurity transport code is left for a future study.

5. Summary

A stable reconstruction method to derive a local SX emissivity was developed. This method are used to study the impurity transport phenomena in LHD device. From these experimental data, a rapid concentration of impurities toward the plasma center has been found in a ice-pellet injected plasma.

References

- [1] S. Yoshimura *et al.*, Fusion Eng. Des. 26, 77 (1995).
- [2] T. Nakagawa and Y. Koyanagi, Data Analysis by Least Square Method (University of Tokyo Press, Tokyo, 1982) p.154 [in Japanese].
- [3] S. Ohdachi *et al.*, Annual Report of National Institute for Fusion Science, 1998-1999, p.10.
- [4] S. Morita *et al.*, Proceedings of 12th International Stellarator Workshop, 1999 Madison, USA.